

# Theory of Materials Formed as Complements of Triply Periodic CMC Surfaces

E. Birgit Kaufmann

Purdue University, Department of Mathematics and Department of Physics and Astronomy

The art of mathematical physics  
in honor of Hubert Saleur's 60th birthday  
Sep 20, 2021

# References

## R. Kaufmann, S. Khlebnikov, and B. K.

- 1 “The geometry of the Double Gyroid wire network: Quantum and Classical”. J. Noncomm. Geom. 6 (2012) 623-664.
- 2 “The noncommutative geometry of wire networks from triply periodic surfaces” J. Phys.: Conf. Ser. 343 (2012), 012054.
- 3 “Singularities, swallowtails and Dirac points. An analysis for families of Hamiltonians and applications to wire networks, especially the Gyroid”. Ann. Phys. 327 (2012) 2865-2884.
- 4 “Projective representations from quantum enhanced graph symmetries”. J. Phys.: Conf. Ser. 597 (2015), 012048.
- 5 “Re-gauging groupoid, symmetries and degeneracies for Graph Hamiltonians and applications to the Gyroid wire network”. Annales Henri Poincaré 17 (2016) 1383–1414

## References II

R. Kaufmann, S. Khlebnikov, and B. K.

- 6 “Singular geometry of the momentum space: From wire networks to quivers and monopoles”. J. Sing. Theory 15 (2016) 53–80
- 7 “Local models and global constraints for degeneracies and band crossings”, J. Geom. and Phys. 158 (2020) 103892-103901

# Background

Initial question by Hugh Hillhouse (then: Chem. Eng. Purdue, now U. of Wash. )

What can mathematicians and physicists tell us about our novel material, which is in the form of a Double Gyroid?  
What follows from its wonderful mathematical structure?

**Hope**  
original motivation: make solar cells more effective  
new prospect: discover special properties driven by topology

**Note**  
We will concentrate on the channels, that is the complementary regions of a fat Gyroid surface.

# Outline

- ① The Double Gyroid
  - The geometric setup
- ② Synthetisation
  - Fabrication
  - Experimental measurements
- ③ Theoretical description and Results
  - Quotient graphs
  - Theoretical description
  - Our Specific Results
- ④ Dirac points and enhanced symmetries
  - Dirac points
  - Enhanced Symmetries
- ⑤ Topological charges and local models
  - Topological charges and local models
  - Setup and Chern classes
  - Slicing
  - Results for the Gyroid



# The Gyroid

## Single Gyroid

- It was discovered by Alan Schoen in 1970.
- It is a triply periodic minimal surface (i.e. surface of constant mean curvature zero)
- It is embedded in  $\mathbb{R}^3$ .
- It appears in nature on wings of certain butterflies and beetles.

## The Double Gyroid (DG)

- The DG interface actually consists of *two* mutually non-intersecting embedded Gyroids.
- The symmetry group is  $Ia\bar{3}d$  where the extra symmetry comes from interchanging the two Gyroids.
- This is the geometry of a thick surface.

# The Double Gyroid

## Level Surface Approximation

- a level surface approximation for the double gyroid is given by the following formula:

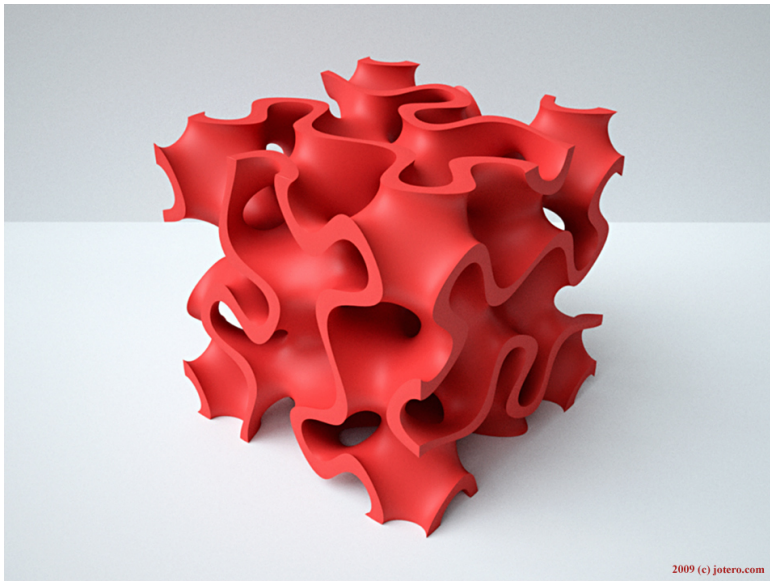
$$L_t : \sin(x) \cos(y) + \sin(y) \cos(z) + \sin(z) \cos(x) = t$$

The double gyroid surface is then modeled by  $L_t$  and  $L_{-t}$  for  $0 < t < \sqrt{2}$ .

## Complement: two channel systems

- The voids in the picture are made up of two non-intersecting channel systems
- we will call these channels  $C_+$  and  $C_-$
- we will concentrate on one of these channels

# The thick or fat surface $F$





# Occurrences in Nature

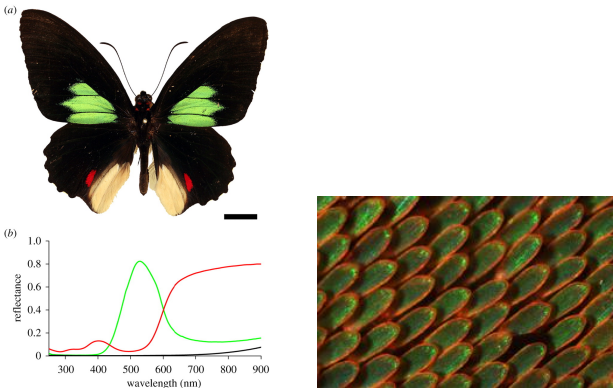


**Figure :** Colored scales on a Papilionid (left hand side: *Parides sesostris*) butterfly wing

# Butterfly Scales

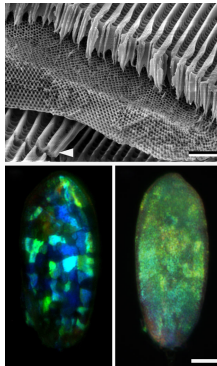


**Figure :** (a) SEM of a fractured scale showing the structural composition of the scale. The approximately 5  $\mu\text{m}$  thick single-network gyroid photonic crystal layer is covered by the approximately 5  $\mu\text{m}$  honeycomb structure, acting as a pigment filter. (b) A single scale upside-down observed through crossed polarizers. (c) A single scale upside up observed through crossed polarizers.



# The two channel systems $C_+$ , $C_-$ : one cell

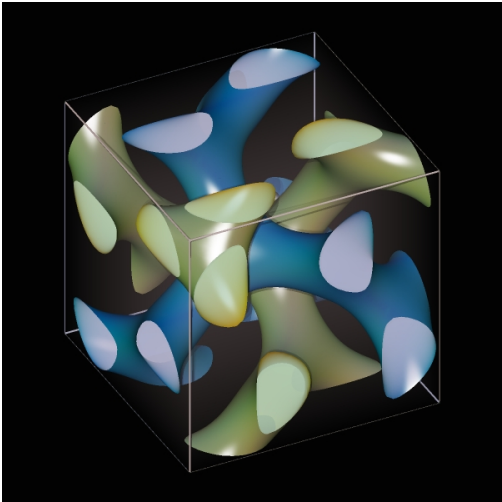


Figure : The two channel systems

# The Channel $C_+$

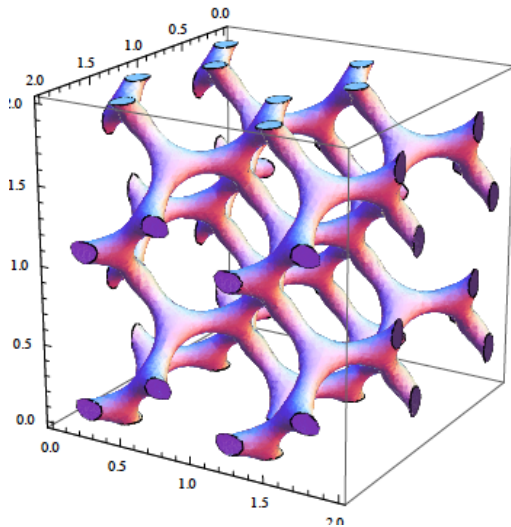


Figure : One channel

# Fabrication

Hugh Hillhouse et al., Purdue, now Univ. of Washington.

- The double-gyroid (DG) is a nanostructure formed by self-assembly in some carefully prepared surfactant or block copolymer systems;
- The cubic lattice constant is 18 nm for the materials of a self-assembled DG structure
- After the first synthesis step, the surfactant is removed yielding a nanoporous silica structure as the fat surface.
- The nanopores (channels) are then filled with a semiconductor (PbSe, PbS, or CdSe) and the silica structure is dissolved to yield the nanowire network.

# Measurements: Eric Stach, while at Purdue, now: BNL

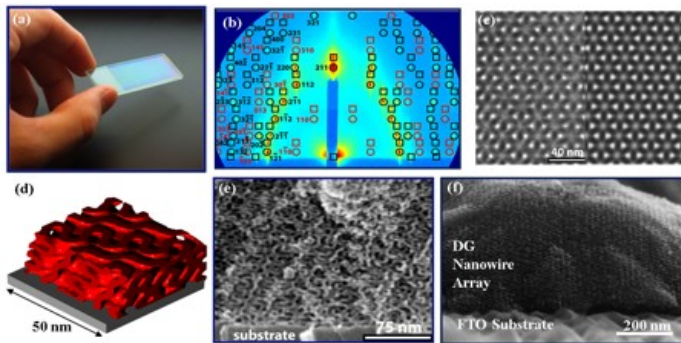
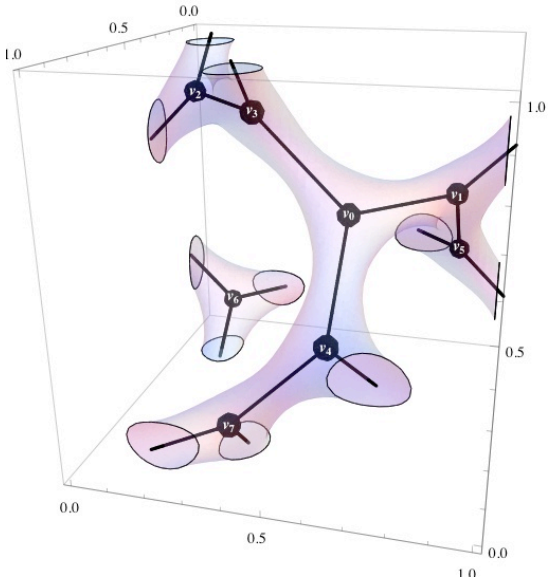
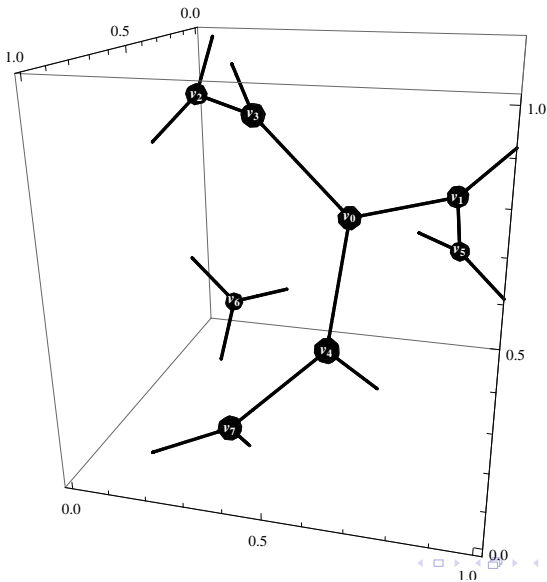


**Figure :** (a) Photograph of DG nanoporous silica film on FTO after self-assembly and surfactant extraction. (b) GISAXS from film showing the high-degree of order and orientation. (c) TEM image of the (111) projection of the DG nanoporous silica film compared with a simulated TEM image for the DG structure. (d) Quantitatively accurate structure of the DG nanoporous silica films determined by GISAXS and TEM. (e) High resolution FESEM image of the cross section of a film. The patterns seen in the structure in panel (d) are easily seen. (f) DG platinum nanowire array obtained by electrodepositing Pt in the DG nanoporous film followed by etching in HF or KOH. Periodic y-junctions can be seen in the nanowires extending from top to bottom through the film.

# The Channel $C_+$ with its skeletal graph $\Gamma_+$



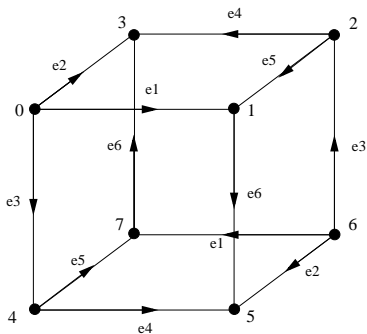
# The skeletal graph $\Gamma_+$



# Quotient Graphs

Quotient by the translational group  $\mathbb{Z}^3 \subset \mathbb{R}^3$

$\Gamma_+/\mathbb{Z}^3$  is a cube. The eight vertices are the images of the vertices  $v_0, \dots, v_7$ .



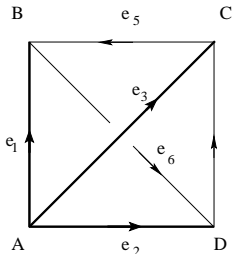
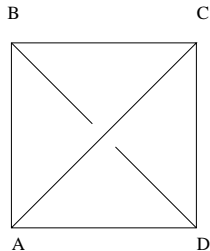
# Topology of $C_+$ or $\Gamma_+$ : finite quotients

Quotient by the full translational symmetry group: bcc

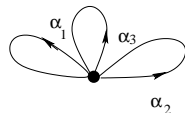
The body centered cubic (bcc) lattice group is generated by  $f_1 := (1, 0, 0)$ ,  $f_2 := (0, 1, 0)$ ,  $f_3 := \frac{1}{2}(1, 1, 1)$ .

$\bar{\Gamma}_+ := \Gamma_+ / \text{bcc}$  is a tetrahedron or full square. This is obtained from the cube by identifying opposite corners

$v_0 \leftrightarrow v_6, v_1 \leftrightarrow v_7, v_2 \leftrightarrow v_4$  and  $v_3 \leftrightarrow v_5$ .



$e_4$



# Theoretical description

## Mathematical formulation

- Define an abstract  $C^*$ -algebra  $\mathcal{B}$  consisting of the Hamiltonian and the symmetries of the system
- The Hamiltonian is the Harper Hamiltonian (tight-binding model)

## Definition

Let  $E$  be the edges of  $\bar{\Gamma}_+$ . Notice that each directed edge defines a unique vector  $\vec{e} \in \mathbb{R}^n$ . Each edge  $e$  defines a set of directed edges and hence two vectors  $\vec{e}, -\vec{e}$ .

The Harper Hamiltonian is  $H = \sum_{e \in E} \hat{T}_{\vec{e}} + \hat{T}_{-\vec{e}}$

In the presence of a magnetic field, these translations do not commute any more.

# Theoretical description

## Mathematical formulation II

- In the presence of a constant magnetic field: algebra becomes non-commutative
- Strategy: study this algebra in both cases, non-commutative and commutative
- Commutative case gives the geometry of the Brillouin zone
- Aim: understand spectrum and physical properties

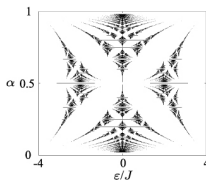
# Our specific results for the Gyroid with magnetic field

## Gap-labelling theorem (with magnetic field)

- If entries of magnetic field are rational, there are only finitely many gaps in the spectrum of  $H$  (analogue of Hofstadter butterfly).
- If entries of magnetic field are irrational, there may potentially be infinitely many gaps

## New measurements

Analogue of Hofstadter butterfly should be measurable in this 3-d system: large lattice constant (18 nm) makes  $B$ -field reasonable



# Our specific results for the Gyroid with magnetic field

## Classification of the algebra $\mathcal{B}$

- The abstract algebra  $\mathcal{B}$  is a subalgebra of a matrix algebra with coefficients in the non-commutative torus.
- At all but finitely many values of the magnetic field, the non-commutative geometry is given by the non-commutative torus
- At special values of the magnetic field (which we can give) the algebra is a proper subalgebra of the non-commutative torus
- At zero magnetic field the commutative geometry is that of a ramified cover of the 3-dimensional torus.
- In this case, we know the level crossing and splittings. Geometrically this is the ramification locus.

# Specific Results without magnetic field

## Dirac points

- In the commutative case (no magnetic field) we found **new Dirac points** for the Gyroid. (Repeating the same analysis for the honeycomb lattice we recover the known Dirac points.)
  - ① We discovered Dirac points in a 3d material, the Gyroid wire network.
  - ② Linear dispersion relation (energy–momentum relation) as for relativistic particles.
- Question: are they topologically stable? Numerical study: yes. Explanation via Chern classes and topological invariants

## Measurements in 3-d material

Dirac points have been measured in similar photonic crystals and other 3-d materials - is it possible to measure them in this structure?

# Hamiltonian for the Gyroid

## Data

- With magnetic field: translations along the edges become magnetic translations, i.e. non-commuting operators  $U_i$  with the relations  $U_i U_j = e^{2\pi i \theta_{ij}} U_j U_i$ ;  $i = 1, 2, 3$
- In Hilbert space decomposition the Graph Harper Operator  $H$  becomes the  $4 \times 4$  matrix

$$H = \begin{pmatrix} 0 & U_1^* & U_2^* & U_3^* \\ U_1 & 0 & U_6^* & U_5 \\ U_2 & U_6 & 0 & U_4 \\ U_3 & U_5^* & U_4^* & 0 \end{pmatrix}$$

- Magnetic Field Parameters:

$$\theta_{12} = \frac{1}{2\pi} B \cdot (g_1 \times g_2), \theta_{13} = \frac{1}{2\pi} B \cdot (g_1 \times g_3), \theta_{23} = \frac{1}{2\pi} B \cdot (g_2 \times g_3)$$

# The Gyroid

## The matrix Harper Operator

$$H = \begin{pmatrix} 0 & 1 & 1 & 1 \\ 1 & 0 & U_1^* U_6^* U_2 & U_1^* U_5 U_3 \\ 1 & U_2^* U_6 U_1 & 0 & U_2^* U_4 U_3 \\ 1 & U_3^* U_5^* U_1 & U_3^* U_4^* U_2 & 0 \end{pmatrix} =: \begin{pmatrix} 0 & 1 & 1 & 1 \\ 1 & 0 & A & B^* \\ 1 & A^* & 0 & C \\ 1 & B & C^* & 0 \end{pmatrix}$$

In the absence of a magnetic field,  $A, B, C$  are commutative and can be written as  $A \mapsto \exp(ia), B \mapsto \exp(ib), C \mapsto \exp(ic)$

# Commutative case

## Basic questions

- ① Classify the points on the base over which the Hamiltonian has degenerate Eigenvalues and give the multiplicities.
- ② If possible identify symmetries, which can correspond to these Eigenspaces

## Answer to Question 1

We answered Question 1 in terms of singularity theory.

## Answer to Question 2

We defined a quasi-classical lift of the classical symmetries of  $\bar{\Gamma}$  on the base space. This also gives rise to a representation of a group extension on  $\mathbb{C}^k$  where  $k = |\bar{\Lambda}|$ .

# New method for analytically finding degeneracies and Dirac points

## Dirac points

- In the commutative case we get a family of Hamiltonians parameterized over a base torus  $T^n$ .
- Consider  $\det(z Id - H(t))$  as smooth function  $P : T^n \times \mathbb{R} \rightarrow \mathbb{R}$ .
- Determine the critical points of  $P$ , viz. singularities.
- The singularity is conical/Dirac if  $P$  has an isolated critical point and the signature of the Hessian is  $(-\cdots - +)$
- Notice we use the embedding of the possibly singular spectrum  $P^{-1}(0)$  into the smooth ambient space  $T^n \times \mathbb{R}$ .

# New method for analytically finding degeneracies and Dirac points

## Characteristic map

Actually  $P^{-1}(0)$  is the pull-back of the miniversal unfolding of the  $A_{k-1}$  singularity along the map given by the coefficients of  $P$  considered as a polynomial in  $z$ . We call that map the characteristic map<sup>a</sup>.

- The characteristic map lets one read off the type of singularities. They are determined by the image and the fiber.
- Singular points are inverse images of the discriminant locus.
- The type of singularity pulled back to the fiber is given by the respective stratum of the unfolding which were determined by Grothendieck.

<sup>a</sup>There is a rescaling involved if  $H(t)$  is not traceless.

# Honeycomb vs. Gyroid:

## Honeycomb

In the case of  $B = 0$  there are two degenerate points in the spectrum, which are cone-like/viz. Dirac. These correspond to enhanced classical symmetries.

## Gyroid

In the case of  $B = 0$  there are four degenerate points in the spectrum. Two of them are triple degeneracies and two of them are two double degeneracies, the latter are cone-like/viz. Dirac. These correspond to enhanced classical symmetries.

# Gyroid and the $A_3$ -Discriminant

The eigenvalues of  $H$  are given by the roots of the characteristic polynomial:  $P(a, b, c, z) = z^4 - 6z^2 + a_1(a, b, c)z + a_0(a, b, c)$

$$a_1 = -2 \cos(a) - 2 \cos(b) - 2 \cos(c) - 2 \cos(a + b + c)$$

$$a_0 = 3 - 2 \cos(a + b) - 2 \cos(b + c) - 2 \cos(a + c)$$

where  $A \mapsto \exp(ia)$ ,  $B \mapsto \exp(ib)$ ,  $C \mapsto \exp(ic)$

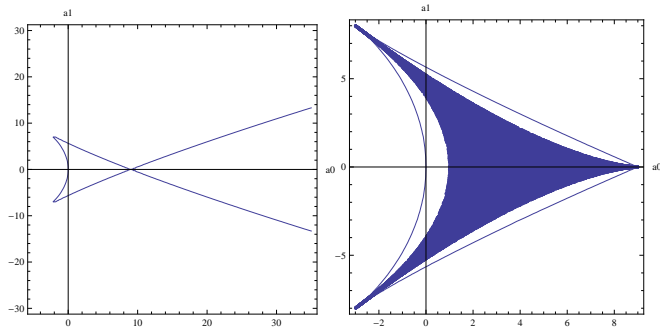


Figure : Discriminant locus (Swallowtail) and region occupied by Gyroid

# $A_3$ singularity and its strata

- Characteristic region contained in the slice of the  $A_3$  singularity with  $a_2 = -6$ , intersects discriminant locus in three isolated points
- two cusps: in stratum of type  $A_2$
- double point: in stratum of type  $(A_1, A_1)$
- fibers over all points are discrete; for  $A_2$  singularities: one point each; for  $(A_1, A_1)$ : two points each; explains crossings in spectrum

# The spectrum of the Gyroid Harper Hamiltonian along the diagonal

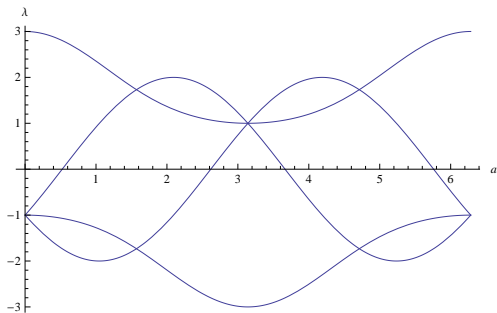


Figure : Spectrum of Harper Gyroid Hamiltonian for  $a = b = c$

# Enhanced Symmetries

## Re-gauging symmetries

- The graph  $\bar{\Gamma}$  has symmetry group  $\mathbb{S}_4$ .
- This action lifts as regaugings on the Hamiltonians by conjugation of matrices.
- The action can be also be lifted to an action on the torus.
- At points with non-trivial stabilizer groups the matrices above give a projective representation of the stabilizer groups.
- The action of  $\mathbb{S}_4$  on  $T^3$  is fixed once we know the action of the generators (12), (23) and (34).
- Both actions can be presented and read off graphically.

# Action of $\mathbb{S}_4$ on $T^3$

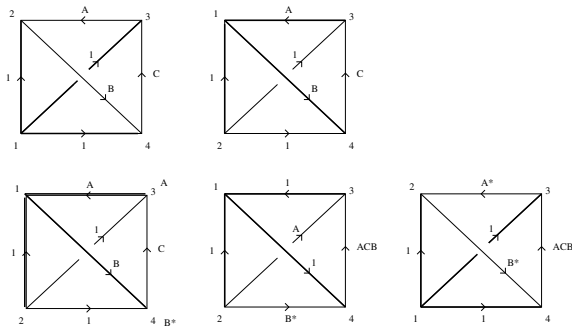


Figure : Calculation of the action of  $(12)$  on  $T^3$

$$(A, B, C) \rightarrow (A^*, B^*, ACB)$$

# The four degenerate points of the Gyroid

## Symmetries at the degenerate points

- The point  $(0, 0, 0)$ . The re-gaugeing matrices give the usual representation of  $\mathbb{S}_4$  on  $\mathbb{C}^4$ , decomposing into the trivial representation and an irreducible 3-dim rep. This leads to one three-fold degenerate eigenvalue.
- The point  $(\pi, \pi, \pi)$ . The re-gaugeing matrices only give a projective representation. We can scale by a 1-cocycle and find again the one-dimensional trivial representation and the 3-dim standard representation.
- The points  $(\frac{\pi}{2}, \frac{\pi}{2}, \frac{\pi}{2})$  and  $(\frac{3\pi}{2}, \frac{3\pi}{2}, \frac{3\pi}{2})$ . We have a projective representation of  $A_4$ . After scaling by a 1-cocycle, we find a representation of  $2A_4$  or binary tetrahedral group. This leads to two eigenvalues with degeneracy 2 (two 2-dim irreps).

# Topological charges: Numerical results

Summary: we explained stability of level sticking analytically with the help of topological invariants/charges and explicit models

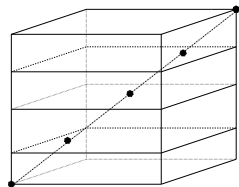
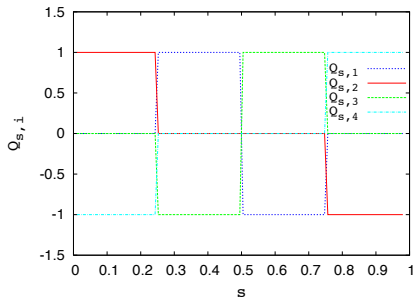


**Figure :** A) Topological charges as functions of the height of a 2-torus slice of the Brillouin zone. The jumps are step functions and the sloped transition is merely a guide. B) The Brillouin torus as a cube with periodic boundaries, the position of the Dirac points and triple crossings along the diagonal and three 2-torus slices.

# Bundle geometry

## Bundle geometry

- Trivial vector bundle  $T \times \mathbb{C}^k \rightarrow \mathbb{C}^k$ ; ( $T = T^d$  is the  $d$ -dimensional torus or Brillouin zone)
- $T_{deg}$  be the locus of points s.t.  $H(t)$  has multiple Eigenvalues.  
 $T_0 := T \setminus T_{deg}$ .

$$\begin{array}{ccc}
 T \times \mathbb{C}^k & \longleftarrow & T_0 \times \mathbb{C}^k \xrightarrow{\sim} \bigoplus_{i=1}^k \mathcal{L}_i \\
 \downarrow & & \downarrow \swarrow \\
 T & \longleftarrow & T_0
 \end{array}$$

- $c_1(\mathcal{L}_i)$  are the charges corresponding to the Berry phases.  
Integral over Berry curvature  $\omega$  [Berry, Simon].

# Bundle geometry

## Bundle geometry

- Trivial vector bundle  $T \times \mathbb{C}^k \rightarrow \mathbb{C}^k$ ; ( $T = T^d$  is the  $d$ -dimensional torus or Brillouin zone)
- $T_{deg}$  be the locus of points s.t.  $H(t)$  has multiple Eigenvalues.  
 $T_0 := T \setminus T_{deg}$ .

$$\begin{array}{ccc}
 T \times \mathbb{C}^k & \longleftarrow & T_0 \times \mathbb{C}^k \xrightarrow{\sim} \bigoplus_{i=1}^k \mathcal{L}_i \\
 \downarrow & & \downarrow \swarrow \\
 T & \longleftarrow & T_0
 \end{array}$$

- $c_1(\mathcal{L}_i)$  are the charges corresponding to the Berry phases. Integral over Berry curvature  $\omega$  [Berry, Simon].
- There are versions for higher degeneracies involving higher Chern-classes. Not today.

# Chern classes

## 2d

If  $T$  is two-dimensional compact. Then the Chern classes are given by  $\int_T \omega$ . This is what happens in the quantum Hall effect. Here  $T = T_0 = T^2$ . Notice that if  $T = T^2$  but  $T_{deg} \neq \emptyset$ , then all  $c_1(\mathcal{L}_i) = 0$ . This is the case for graphene  $\leadsto$  Dirac points not topologically protected.

## 3d

The Chern classes are determined by their pairing with  $H_2(T_0, \mathbb{Z})$ . If  $T = T^3$  there is nice method to encode this using slicing.

# Slicing

## Setup

- $\pi_i : T^3 = S^1 \times S^1 \times S^1 \rightarrow S^1$  the  $i$ -th projection.
- $\iota(t) : T^2 = S^1 \times S^1 \rightarrow T^3 = S^1 \times S^1 \times S^1$  inclusion  $(t_1, t_2) \mapsto (t_1, t_2, t)$ .
- $c_1^i(t) := \int_{T^2} \iota(t)^* c_1(\mathcal{L}_i)$  for  $t \notin \pi_3(T_{deg})$ .
- For  $t \in \pi_3(T_{deg})$  set  $c_1^i(t) := 0$ . This is also the result of pulling back the Chern class to  $T^2 \setminus \iota(t)^{-1}(T_{deg})$ .
- There are of course similar definitions for the other two inclusions and higher dimensions.



# Chern jumps and local charges

## Local charges/jumps

$T$  three dimensional,  $p$  isolated point in  $T_{deg}$ . The local charges at  $p$  are  $c_1^i(p) = \int_{S^2(p)} c_1(\mathcal{L}_i)$  where  $S^2(p)$  is a little sphere centered at  $p$ .

A local model (Berry, Simons, ...) in 3d for an isolated  $2k + 1$ -dimensional crossing

$H(\mathbf{x}) := \mathbf{x} \cdot \mathbf{L} = xL_x + yL_y + zL_z$  where  $L_{x,y,z}$  is a  $k$  dimensional representation of spin  $m$ .

The local charges are  $c_1^i \in \{-m, \dots, m\}$ .



# Questions

## Local models

For a double crossing/Dirac point, the above model is the only model. What are the other local models for higher degeneracies? Phase diagram?

## Global properties

- 1 Depending on properties of  $H(t)$  can one say something directly about the  $\mathcal{L}_i$  or the  $c^i$ ?
- 2 How much does this determine them? Examples:  
 $\sum_i c_1^i(t) \cong 0$  always.  
 If there is time reversal symmetry  $c_1^i(t) = -c_1^i(-t)$ .
- 3 How much does knowing the local models determine the global structure?
- 4 What is the behavior under perturbations?

# Spin type model

## Definition of spin type model

We say that an isolated point  $\mathbf{k}_0 \in T_{deg}$  is of spin type  $(s_1, \dots, s_l)$ , if it is of singularity type  $(A_{2s_1}, \dots, A_{2s_l})$  and there is a linear isomorphism  $L_{\phi_j}$  for each  $A_{k_j}$  singularity in the Eigenvalues to first order perturbation theory

$$P_j[H(\mathbf{k}_0 + \mathbf{x}) - H(\mathbf{k}_0)]P_j = \mathbf{a}_j \mathbf{x} \text{ id} + L_{\phi_j}(\mathbf{x}) \cdot \mathbf{S} + O(\mathbf{x}^2)$$

where  $\mathbf{a}_j$  is a vector,  $\mathbf{S} = (S_x, S_y, S_z)$  is a spin  $s_j$  representation of  $su(2)$  and  $P_j$  is the projector onto the degenerate Eigenspace of the  $2s_j + 1$  fold crossing.

## local charges and chirality

local charges:  $2m \text{ sign}(\det(L_{\phi_j}))$  where  $m = -s_j, \dots, s_j$

The sign  $\text{sign}(\det(L_{\phi_j}))$  is independent of  $m$  and will be called the *chirality*.

# Results for the Gyroid

## local spin type models

Using perturbation theory, we can show that all level crossings are of spin type:

- 1 The point  $(0, 0, 0)$  is of spin type  $(1, 0)$  with the chirality 1.
- 2 The point  $(\pi, \pi, \pi)$  is of spin type  $(0, 1)$  with chirality  $-1$ .
- 3 The point  $(\frac{\pi}{2}, \frac{\pi}{2}, \frac{\pi}{2})$  is of spin type  $(\frac{1}{2}, \frac{1}{2})$  with chirality  $(-1, 1)$ .
- 4 The point  $(\frac{3\pi}{2}, \frac{3\pi}{2}, \frac{3\pi}{2})$  is of spin type  $(\frac{1}{2}, \frac{1}{2})$  with chirality  $(-1, 1)$ .

# Global constraints

## global constraints

There are three different types of global constraints:

- 1 global constraints for the slicing charges  $c_1^i(t)$ . E.g. they are locally constant outside of the singular points and step functions with integer values.
- 2 global constraints from time reversal symmetry, e.g.  $c_1^i(t) = -c_1^i(-t)$
- 3 The Gyroid exhibits an extra symmetry given by  $H(\mathbf{k} + (\pi, \pi, \pi)) = U^\dagger(-H(\mathbf{k}))U$  with  $U = \text{diag}(-1, 1, 1, 1)$ . This means singularities translated by  $(\pi, \pi, \pi)$  are related and of opposite chirality.

# Results

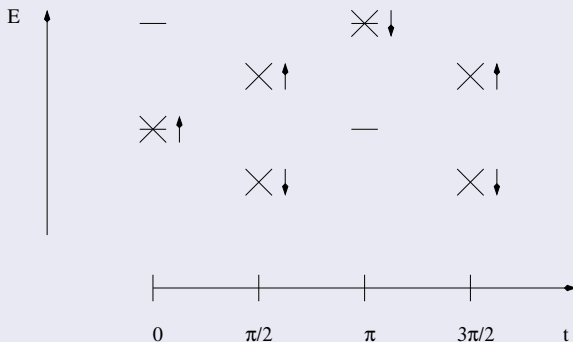


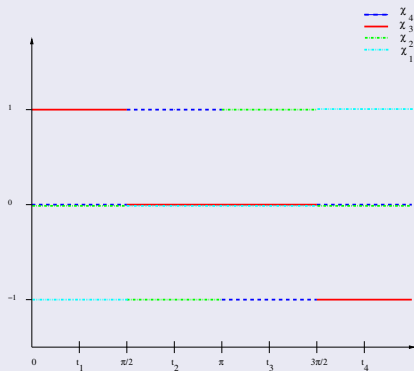
**Figure :** Schematic of the singularities for the  $z$  slicing. Single lines are of type  $A_0$ , i.e. no crossing. Crosses indicate  $A_1$  Dirac points. These are spin  $1/2$ . The  $A_2$  triple crossings are of spin  $1$  type. The chiralities are indicated by arrows.  $\uparrow$  means  $+1$  and  $\downarrow$  means  $-1$  chirality. The axes are the slicing parameter  $t$  and the energy  $E$ . The latter is only schematic, to indicate the relative positions of the level.

## Results

Gyroid: level crossings completely characterized

Change of notation:  $\chi_i(t) = c_1^i(t)$ 

	$t_1$	$t_2$	$t_3$	$t_4$
$\chi_1$	-1	0	0	1
$\chi_2$	0	-1	1	0
$\chi_3$	1	0	0	-1
$\chi_4$	0	1	-1	0

Figure : Values of the functions  $\chi_i$  and graphs

# Results

## Gyroid: level crossings completely fixed up to one parameter

Due to TRS and the extra symmetry, the chiralities of the  $(\frac{1}{2}, \frac{1}{2})$  spin type points are fixed by the chirality of one of the double crossings. Given this chirality,  $\chi_1$  and  $\chi_4$ ,  $\chi_2$  and  $\chi_3$  are fixed up to a parameter.

## Relevance

In this case everything can be calculated by perturbation theory, but the power of our method becomes evident if we deform the Hamiltonian.

# Stability of Dirac points

## Symmetry breaking deformations

Numerical study: introducing symmetry breaking deformations in the Hamiltonian; keeping time reversal symmetry

$$H_d = \begin{pmatrix} V_1 & 1 & 1 & 1 \\ 1 & V_2 & A & B^* \\ 1 & A^* & V_3 & C \\ 1 & B & C^* & V_4 \end{pmatrix}$$

with  $A = r_a e^{ia}$ ,  $B = r_b e^{ib}$ ,  $C = r_c e^{ic}$ , where  $V_i, r_a, r_b, r_c$  are real randomly generated numbers; distributed around their ideal values within a few percent.

# Stability of Dirac points

## Symmetry breaking deformations

- Results: Dirac points are stable under these deformations; results from previous explanation via Chern classes
- triple crossings break up into four double crossings
- we see this numerically; we can explain it again by time-reversal symmetry and global constraints
- in fact, the numerical picture is the minimal resolution of the constraints worked out analytically

# Plot for deformed case

## Deformed case

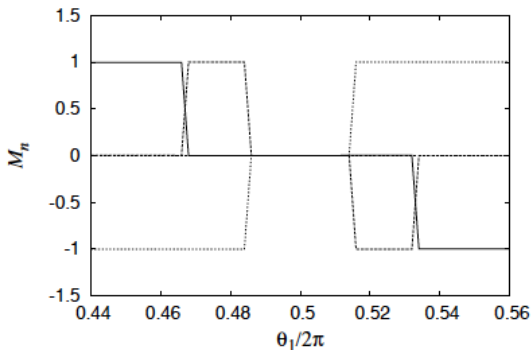


Figure : Slicing along  $z$  numerically near the old triple crossing at  $(\pi, \pi, \pi)$ . This breaks up into *four*  $A_1$  points

# Conclusion

Gyroid is most interesting of triply periodic structures (compared to P and D)

- Interesting topology at the singular points in the band structure
- topological properties can be explained analytically
- can be viewed as 3-d analogue of graphene: two Dirac points
- we developed local and global models to explain the level crossings
- stable under deformations, so they should be present in real material
- with sophisticated experimental techniques: they should be observable

## Other triply periodic wire networks

There are only three (families) of triply periodic minimal surfaces whose complements are given by symmetric and self-dual graphs (1) the P or primitive or cubic surface, (2) the D or diamond surface and (3) the G or gyroid surface.

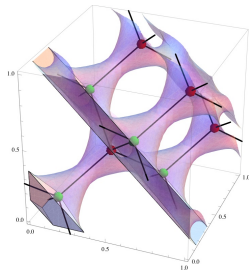
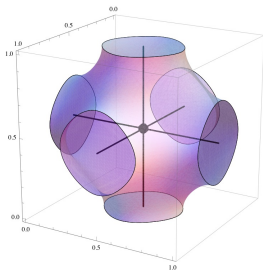


**Figure :** One channel of the P surface and of the diamond surface and their skeletal graph. The red and green dots refer to the vertices of the two interlaced fcc lattices

# The end

Thank you!

# Enhanced Symmetries

## Re-gauging symmetries

- The Gyroid graph  $\Gamma_+$  is a graph in  $\mathbb{R}^3$  with bcc symmetry.
- Its quotient by bcc,  $\bar{\Gamma}_+$ , is the tetrahedron. This is the graph of interest for the present discussion.
- It has symmetry group  $\mathbb{S}_4$ .
- This action lifts as regaugings on the Hamiltonians by conjugation of matrices.
- The action can be also be represented by an action on the base torus  $T^3$  ( $\widetilde{Arc} = C^*(T^3)$ ).
- At points with non-trivial stabilizer groups the matrices above give a projective representation of the stabilizer groups.
- The action of  $\mathbb{S}_4$  on  $T^3$  is fixed once we know the action of the generators (12), (23) and (34).
- Both actions can be presented and read off graphically.

# Action of $\mathbb{S}_4$ on $T^3$

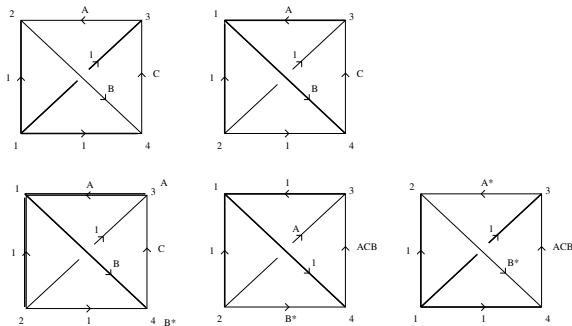


Figure : Calculation of the action of  $(12)$  on  $T^3$

$$(A, B, C) \rightarrow (A^*, B^*, ACB)$$

# The four degenerate points of the Gyroid

## Symmetries at the degenerate points

- The point  $(0, 0, 0)$ . The re-gaugeing matrices give the usual representation of  $\mathbb{S}_4$  on  $\mathbb{C}^4$ , decomposing into the trivial representation and an irreducible 3-dim rep. This leads to one three-fold degenerate eigenvalue.
- The point  $(\pi, \pi, \pi)$ . The re-gaugeing matrices only give a projective representation. We can scale by a 1-cocycle and find again the one-dimensional trivial representation and the 3-dim standard representation.
- The points  $(\frac{\pi}{2}, \frac{\pi}{2}, \frac{\pi}{2})$  and  $(\frac{3\pi}{2}, \frac{3\pi}{2}, \frac{3\pi}{2})$ . We have a projective representation of  $A_4$ . After scaling by a 1-cocycle, we find a representation of  $2A_4$  or binary tetrahedral group. This leads to two eigenvalues with degeneracy 2 (two 2-dim irreps).





# Results on P and D

## P surface

This is just the case of  $\mathbb{Z}^3$ . The abstract algebra is just the 3-torus. There is only one Eigenvalue and hence no degeneracies for  $B = 0$ . No Dirac points!

## D surface

The locus where the algebra  $\mathcal{B}_\Theta$  is not the full matrix algebra is given by three one dimensional families — again parameterized by the magnetic field parameters. And several special points corresponding to bosonic and fermionic cases.

The locus of degenerate Eigenvalues in the case  $B = 0$  is given by three circles which pairwise touch at a point given by the equations  $\phi_i = \pi, \phi_j \equiv \phi_k + \pi \pmod{2\pi}$  with  $\{i, j, k\} = \{1, 2, 3\}$ . No Dirac points!

# Conclusion

Gyroid is most interesting of triply periodic structures (compared to P and D)

- Interesting topology at the singular points in the band structure
- topological properties can be explained analytically
- large lattice constant:  $B$ -field manageable
- can be viewed as 3-d analogue of graphene: two Dirac points
- stable under deformations, so they should be present in real material
- with sophisticated experimental techniques: they should be observable

# The end

Thank you!